https://doi.org/10.3311/PPch.42875

Periodica Polytechnica Chemical Engineering

Application of Naturally Derived Surfactant from Chickweek and Titanium Dioxide Nanoparticles for Improving Oil Recovery in a Carbonate Reservoir

Saeid Alamdari[1], Moein Nabipour[1*], Amin Azdarpour[1], Bizhan Honarvar[1], Nadia Esfandiari[1]

[1] Department of Chemical Engineering, Marv. C., Islamic Azad University, Marvdasht, Iran
[*] Corresponding author, e-mail: nabipour@gmail.com

Received: 23 November 2025, Accepted: 27 March 2026, Published online: 18 May 2026

Abstract

This study investigates the interfacial performance and enhanced oil recovery (EOR) potential of a naturally derived surfactant extracted from chickweed in combination with titanium dioxide nanoparticle under harsh reservoir conditions. A comprehensive experimental program was conducted to characterize the chemical structure, stability and interfacial activity of the formulated system using spectroscopic analyses, interfacial tension measurements, wettability evaluation and core flooding tests. Results demonstrate that the chickweed-derived surfactant exhibits strong amphiphilic characteristics and maintains compatibility with high-salinity formation brine and nanoparticles over prolonged ageing at elevated temperature. The hybrid formulation significantly reduced oil–water interfacial tension, shifted carbonate rock wettability toward a more water-wet state and improved microscopic displacement efficiency. Core flooding experiments confirmed a measurable incremental oil recovery compared with conventional waterflooding, highlighting the combined role of interfacial tension reduction, wettability alteration and improved dispersion stability. The findings suggest that chickweed-based surfactants, particularly when integrated with metal-oxide nanoparticles, represent a promising environmentally conscious alternative for chemical EOR applications in high-salinity carbonate reservoirs.

Keywords

chickweed, natural surfactant, Nano-TiO_2, EOR, oil recovery factor

1 Introduction

The continuous growth in global energy demand, coupled with the progressive depletion of easily recoverable hydrocarbon resources, has intensified the need for more efficient and sustainable enhanced oil recovery (EOR) strategies. A significant proportion of original oil in place remains trapped after primary and secondary recovery due to capillary forces, unfavorable wettability and reservoir heterogeneity. Among chemical EOR methods surfactant flooding has attracted considerable attention because of its ability to reduce interfacial tension (IFT) and alter rock wettability, thereby mobilizing residual oil. However, the environmental concerns, high cost and salinity sensitivity associated with many conventional synthetic surfactants have driven increasing interest toward bio-derived alternatives. In this context plant-based natural surfactants, particularly those rich in saponins, offer a promising pathway due to their biodegradability, surface activity, and compatibility with harsh reservoir conditions. Integrating such sustainable materials with nanotechnology further opens new opportunities to enhance stability and interfacial performance, motivating the present investigation [1–6].

Bio-surfactants and other green surface-active agents have emerged as versatile materials across a wide range of industrial and environmental applications due to their low toxicity, biodegradability and ability to function under harsh conditions. In the petroleum sector they are increasingly explored for EOR, drilling fluid formulation and produced-water treatment, where their capacity to reduce interfacial tension and modify wettability can improve displacement efficiency while minimizing ecological impact. Beyond energy applications bio-surfactants are widely utilized in environmental remediation for the mobilization of hydrophobic contaminants, as well as in pharmaceuticals, cosmetics, agriculture and food processing, where mildness and biocompatibility are essential. Their performance in high salinity and temperature environments,

Cite this article as: Alamdari, S., Nabipour, M., Azdarpour, A., Honarvar, B., Esfandiari, N. "Application of Naturally Derived Surfactant from Chickweek and Titanium Dioxide Nanoparticles for Improving Oil Recovery in a Carbonate Reservoir", Periodica Polytechnica Chemical Engineering, 2026.
https://doi.org/10.3311/PPch.42875

coupled with growing regulatory pressure to replace petroleum-derived chemicals, positions green surfactants as sustainable alternatives that can bridge performance requirements with environmental stewardship [7–10].

Recent research has increasingly focused on the development of bio-derived surfactants as sustainable alternatives to conventional petroleum-based chemicals in chemical EOR. In this context, an anionic surfactant synthesized from peanut oil has demonstrated promising performance, highlighting the viability of plant-based feedstocks for EOR formulations. The surfactant, produced via esterification followed by sulfonation, was structurally validated using Fourier transform infrared (FTIR), ^{1}H-NMR and thermogravimetric analyses, confirming the successful incorporation of functional groups responsible for surface activity. Physicochemical evaluation through conductivity and surface tension measurements identified an optimal critical micelle concentration with 2000 ppm, which was subsequently used to assess interfacial and displacement performance. At this concentration the formulation achieved an ultralow interfacial tension on the order of 10^{-2} mN/m under moderate salinity, while also inducing a pronounced wettability shift from strongly oil-wet to water-wet conditions in both sandstone and carbonate substrates. Complementary tests further revealed strong emulsification capacity and long-term emulsion stability under saline environments, indicating favorable phase behavior and compatibility. Core flooding experiments corroborated these interfacial improvements, showing measurable incremental recoveries exceeding 15–19% of the original oil in place and a beneficial shift in relative permeability characteristics. Collectively these findings reinforce the growing evidence that plant-derived surfactants can deliver competitive technical performance while aligning with environmental and sustainability objectives, thereby motivating continued exploration of green surfactant systems for EOR applications [11].

Recent investigations have explored plant-derived saponins as environmentally benign surfactants for chemical EOR. In one such study, purified saponin extracted from Prosopis farcta was systematically evaluated after structural confirmation using FTIR, thermogravimetric (TGA) and ^{1}H-NMR analyses, which verified its molecular integrity and thermal robustness. The surfactant exhibited a well-defined critical micelle concentration at approximately 3000 ppm based on conductivity and surface tension trends. At this concentration the formulation significantly reduced oil-water interfacial tension, with further improvement observed in the presence of salinity, indicating favorable performance under reservoir-relevant conditions. Wettability measurements demonstrated effective alteration of both sandstone and carbonate substrates toward more water-wet states, while foamability and emulsification tests confirmed the ability of the saponin to generate stable dispersed systems. Core flooding experiments further substantiated its displacement capability, yielding measurable incremental recoveries in both lithologies relative to conventional water injection. Collectively these findings highlight the promise of plant-extracted saponins as viable low-toxicity alternatives for improving microscopic displacement efficiency in diverse reservoir environments [12].

Recent studies have explored hybrid chemical-nanotechnology strategies to overcome the limitations of conventional chemical EOR processes, particularly their inefficiency in mobilizing residual oil within complex pore structures. One investigation assessed wettability modification of carbonate rocks using synthesized SiO_2/KCl/xanthan nanocomposites in combination with mutual solvents such as ethanol and methyl ethyl ketone. The results demonstrated that the rock surface behavior was strongly governed by the fluid salinity and the solvent composition. While reducing the salinity of the base brine alone led to lower contact angles, the addition of solvents reversed this trend, with higher salinity producing greater wettability alteration. Increasing solvent concentration further enhanced this effect, indicating a synergistic role between polarity modification and interfacial interactions. The hybrid smart-water/solvent/nanocomposite formulation achieved the most pronounced shift toward water-wet conditions, reducing the contact angle from approximately 125° to about 39°. Core displacement tests confirmed the macroscopic impact of this wettability control, where optimized solvent-brine mixtures delivered substantial reductions in residual oil saturation with recovery improvements exceeding 50% of original oil in place (OOIP). These findings underscore the potential of integrating nanoparticles and mutual solvents with tailored brine chemistry to amplify the interfacial modification and improve the displacement efficiency in carbonate reservoirs [13].

Recent work has examined plant-derived surfactants as ion-tunable agents for improving interfacial properties in carbonate reservoirs. In one investigation, natural surfactants extracted from hop and dill were evaluated for their ability to modify fluid-fluid and rock-fluid interactions. Experimental results demonstrated significant reductions in oil-water interfacial tension with values decreasing from roughly 28 mN/m to the low single-digit range depending on the surfactant type. Salinity optimization further

enhanced the performance with an intermediate ionic strength providing the most effective interfacial response. Wettability measurements confirmed a pronounced shift toward more water-wet conditions, evidenced by substantial decreases in contact angle, while zeta potential analysis supported the observed surface charge modifications. Dynamic core flooding experiments corroborated these microscopic observations, showing measurable incremental oil recovery during both secondary and tertiary injection stages. Collectively, the study illustrates that ion-tuned natural surfactants can deliver simultaneous IFT reduction and wettability control, reinforcing their potential as environmentally compatible alternatives for improving recovery efficiency in carbonate formations [14].

A growing body of research has also investigated bio-derived polymers as mobility-control agents in chemical EOR. In one study, an aloe-based biopolymer was evaluated as a sustainable alternative to conventional synthetic polymers, demonstrating favorable thermal stability and strong compatibility with high-salinity formation brines (FBs). The polymer performance was further examined in combination with a KCl/SiO_2/xanthan nanocomposite, forming a hybrid chemical formulation aimed at improving both interfacial properties and sweep efficiency. Experimental observations revealed that solvent addition moderately reduced interfacial tension and contact angle, whereas incorporating the nanocomposite produced a much stronger effect, indicating a synergistic interaction between the polymer matrix and nanoparticles. Rheological analysis confirmed predictable flow behavior suitable for reservoir injection, while core flooding experiments showed substantial enhancement in oil recovery, attributed to simultaneous mobility control, wettability alteration, and interfacial tension reduction. These findings highlight the potential of integrating biopolymers with nanostructured additives to achieve environmentally compatible and technically effective recovery strategies [15].

While the synergistic use of plant-derived saponins with nanoparticles and divalent ions has been previously reported (the summary is shown in Table 1 [16–27]), the present work advances the field through several clearly defined differentiators. First, it provides a chemical and functional fingerprint of a chickweed-derived surfactant, a biosource that has received minimal attention in EOR literature compared with more commonly studied saponin extracts. Second, the formulation is systematically evaluated under ultra-high salinity conditions (total dissolved solids, TDS ≈ 97,645 ppm) representative of harsh carbonate reservoirs, establishing a well-defined compatibility and stability window at 80 °C through extended ageing and physicochemical analyses. Third, the study demonstrates the specific interfacial and transport behavior of the chickweed-titanium dioxide nanoparticle (Nano-TiO_2) system in the presence of divalent ions, clarifying how stability and dispersion are preserved at high ionic strength. Finally, the work links these mechanistic observations to quantified incremental oil recovery under a controlled coreflooding protocol, providing a direct performance benchmark rather than relying solely on interfacial metrics. Collectively, these aspects move beyond generic "plant surfactant and nanoparticle" synergy and establish a reservoir-relevant, mechanistically supported formulation framework.

Table 1 Summary of previous studies on natural surfactants for EOR applications

Raw material	Surfactant type	CMC* (ppm)	Ref.
Jatropha oil	Anionic	8000	[16]
Palm oil	Anionic	4500	[17]
Sapindus laurifolius	Anionic	9000	[18]
Palm oil	Anionic	8000	[19]
Quinoa plant	Nonionic	1500	[20]
Avena sativa	Nonionic	4000	[21]
Pisum sativum	Nonionic	1500	[22]
Acacia concinna	Nonionic	1500	[23]
Waste cooking oil	Zwitterionic	4000	[24]
Cardanol	Zwitterionic	300	[25]
Castor oil	Polymeric	5000	[26]
Jatropha oil	Polymeric	6000	[27]

* Critical micelle concentration

2 Materials and methods

2.1 Materials

Dried chickweed, as shown in Fig. 1, was used as the raw material for saponin extraction in this study. Fresh plants were first washed thoroughly to remove soil and surface impurities, then air-dried under shade conditions to preserve thermally sensitive compounds. The dried material was ground into a fine powder using a laboratory mill to increase surface area and improve the solvent penetration during extraction. This powdered chickweed served as the feedstock for subsequent ethanol-water solvent extraction of saponins, ensuring consistency and reproducibility of the natural surfactant preparation.

In addition, Nano-TiO_2 was purchased locally (Amin Petro Zagros Zand Company, Iran) and used in this study. After purchasing the Nano-TiO_2 powder, additional

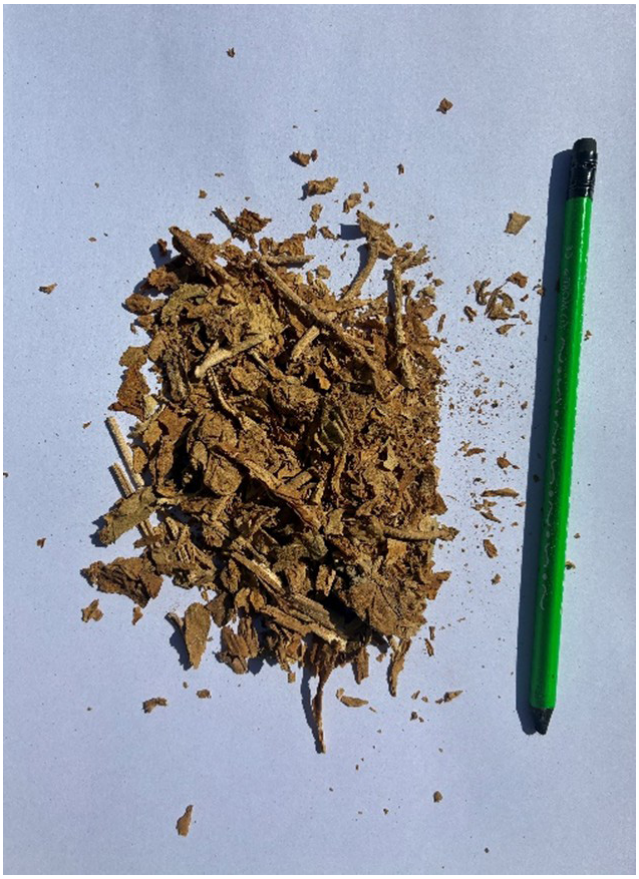

Fig. 1 Image of dried chickweed used in this study

characterization to better understand its properties before using it in the flooding experiments were performed. The particle size distribution in aqueous media was evaluated by dynamic light scattering (DLS) (Malvern Instruments, Malvern, UK) in order to check the dispersion quality and identify any possible aggregation. In addition, the specific surface area of the nanoparticles was determined from nitrogen adsorption–desorption measurements based on the Brunauer–Emmett–Teller (BET) method. These analyses allowed us to confirm that the particles were within the nanoscale range and possessed a sufficiently high surface area, which is important for their interaction with surfactant molecules and their performance in interfacial tension reduction and wettability alteration.

To minimize the potential risks associated with nanoparticle transport in porous media, including retention, aggregation, and pore throat blockage, several precautionary measures were incorporated into the experimental design. The Nano-TiO_2 dispersions were first sonicated for 30 min to break down weak agglomerates and ensure uniform particle distribution prior to injection. All nanofluids were prepared at concentrations below the threshold typically associated with permeability impairment, and their stability was verified through visual inspection and particle size consistency before coreflooding. In addition, the injection sequence was conducted at moderate flow rates to limit mechanical trapping and reduce the likelihood of particle accumulation at pore constrictions. Permeability was monitored before and after flooding to confirm that no significant formation damage occurred within the duration of the experiments. While these steps reduce the probability of adverse effects under laboratory conditions, it is acknowledged that long-term nanoparticle retention and scale-up behavior may vary under field conditions, and therefore warrant further investigation.

A crude oil sample with an API gravity of 31.56° was obtained from a reservoir in southern Iran and used throughout this study. Saturates, aromatics, resins, and asphaltenes (SARA) characterization indicated that the oil consisted of 53.35 wt% saturates, 32.28 wt% aromatics, 9.78 wt% resins, and 4.59 wt% asphaltenes. Furthermore, the measured acid number (AN) and base number (BN) were 1.63 and 0.46, respectively.

Carbonate core plugs used in this study were collected from outcrop intervals of a carbonate reservoir in Iran. Petrophysical properties were determined using helium porosimetry for porosity and brine flow tests for permeability. The samples exhibited porosity values in a narrow range of 11.26–11.33%, while permeability varied from 14.87 to 14.98 mD.

Mineralogical characterization by Xray diffraction (XRD) revealed that the rock matrix is dominated by calcite (50%), followed by dolomite (33%), with the remaining 17% comprising minor mineral phases.

For the experimental procedures, formation brine with a TDS concentration of 97,645 ppm was collected from the same field and used as the base aqueous phase. In addition, synthetic brines were formulated using analytical-grade $MgCl_2$, NaCl, and KCl (Merck, Germany) salts with a stated purity of 99%, procured from local suppliers.

2.2 Extraction of saponin from chickweed

The saponin extraction was carried out following the protocol established in our previous studies [20, 23, 28]. In brief, 100 g dried chickweed powder was loaded into a Soxhlet apparatus, and 500 mL methanol was cycled for approximately 10 h. The methanolic extract was concentrated via rotary evaporation to remove the solvent, yielding the crude surfactant fraction.

The residue was then combined with 50 mL distilled water in a separatory funnel, followed by the addition of

50 mL n-butanol. The mixture was stirred for about 2 h to achieve phase separation. The n-butanol layer, containing the target organic compounds, was collected and concentrated again using a rotary evaporator.

Subsequently, diethyl ether was added to the concentrated extract, and the solution was centrifuged at 3500 rpm for 20 min. The final product obtained after solvent partitioning and solvent removal is referred to as a partially purified saponin-rich fraction, as the procedure enriches surface-active glycosides while not targeting isolation of individual saponin molecules.

The total saponin content of the chickweed extract was quantified using a UV–Vis colorimetric method based on the formation of a chromogenic complex between saponins and vanillin-sulfuric acid reagent. Briefly, a known mass of the dried extract was dissolved in aqueous ethanol (water/ethanol ratio: 1:1), and an aliquot of the solution was reacted with freshly prepared vanillin reagent followed by concentrated sulfuric acid under ambient temperature [20]. After cooling to room temperature, the absorbance was measured at the characteristic wavelength using a UV–Vis spectrophotometer (where the wavelength was 400 to 800 nm, and the linear range of the calibration was 0 to 150% of the expected analyte concentration). A calibration curve was constructed using standard saponin solutions, and the saponin concentration in the extract was calculated from the linear regression equation. The results were reported as weight percent of saponin relative to the dry extract mass, providing a quantitative measure of surfactant purity prior to formulation.

To evaluate extraction reproducibility, the saponin extraction procedure was repeated in three independent batches under identical operating conditions, including solvent ratio, extraction time, and temperature. The extraction yield and saponin content of each batch were determined and compared. The relative standard deviation (RSD) of the measured values was calculated to assess consistency between batches. The low variability observed among the replicates confirms that the extraction protocol provides reliable and repeatable production of chickweed-derived surfactant suitable for subsequent physicochemical and EOR experiments.

2.3 Characterization of saponin

The extracted saponin was characterized using a suite of analytical techniques, including ^{1}H NMR and FTIR spectroscopy. For structural analysis, the surfactant was dissolved in DMSO-d_6 and examined on a Bruker 500 MHz spectrometer at 25 °C, providing detailed proton NMR information. Functional groups and molecular bonding environments were assessed via FTIR spectroscopy using a VARIAN Inova instrument (USA) over the 500–4000 cm^{-1} spectral range.

2.4 IFT and contact angle measurement

IFT measurements between various solutions and crude oil under reservoir conditions were carried out using the IFT400 apparatus (Fars EOR Tech. Co., Iran). This system utilizes the pendant drop method coupled with axisymmetric drop shape analysis (ADSA), as described in previous studies [29, 30]. The instrument can operate at pressures up to 41368 kPa and temperatures up to 204.4 °C. In this approach, IFT (γ, mN/m) is calculated using the proper equation:

$$\gamma = \Delta\rho g D^{2/H}, \tag{1}$$

where $\Delta\rho$ is the density difference between the fluids, g is the gravitational acceleration, D is the drop's maximum diameter, and H is the shape factor. Drop images are captured and analyzed via ADSA to determine the IFT values, with an experimental uncertainty of ±5%. Measurements in this work were performed at 80 °C for the prepared solutions.

The impact of these solutions on rock wettability was evaluated using the contact angle method. Rock slices were pre-saturated with oil for 40 days at 80 °C to shift their surface from water-wet to oil-wet. Contact angles were then measured via the sessile drop technique using the same IFT400 instrument, under 80 °C and atmospheric pressure. Measurements were recorded over periods up to 195 h, with each test performed in triplicate and the median value reported to reduce experimental variability. Both left and right contact angles of each droplet were measured, and their average was used as the final contact angle for each test.

2.5 Oil recovery factor measurement

Oil recovery experiments in this study were conducted using a core flooding system (Fars EOR Co., Iran). The apparatus consists of three 500 mL fluid accumulators, a stainless-steel core holder, an HPLC pump, a hand-operated pump for confining pressure, a gas back-pressure regulator (400 bar), an oven for temperature control, and a differential pressure measurement unit. Both produced oil volumes and pressure differentials were continuously monitored throughout the experiments. The core flooding procedure, adapted from previous work [21, 31], was carried out as follows:

Core samples were cleaned sequentially with toluene and acetone. The cleaned cores were dried overnight at 70 °C, with weights recorded before and after drying.

Each core was placed in a saturator, evacuated under vacuum for 1 h, and then saturated with formation brine at 24.13 MPa for 24 h. The cores were mounted in the core holder, and 5 pore volume (PV) of formation brine was injected at 80 °C and 31.03 MPa to establish equilibrium. Approximately 5 PV of dead oil was injected to reach residual water saturation under the same temperature and pressure conditions. To restore original wettability and equilibrate the rock-brine-oil system, cores were aged in crude oil at 80 °C for about one month. Secondary recovery was performed by injecting 5 PV of formation brine at 80 °C and 31.03 MPa. Tertiary recovery involved 5 PV of a solution containing 4000 ppm natural surfactant in formation brine at a flow rate of 3×10^{-7} m^3/min. The tertiary recovery procedure was repeated using a solution containing 4000 ppm natural surfactant and 2000 ppm NanoTiO_2.

3 Results and discussions

3.1 Characterization of Nano-TiO_2

DLS measurements, as shown in Fig. 2, were conducted to evaluate the particle size distribution of Nano-TiO_2 after dispersion in deionized water (DIW). The results indicated a relatively narrow size distribution centered around approximately 30 nm, confirming that the particles remained within the nanoscale range after sonication. No significant secondary peaks were observed, suggesting that large-scale aggregation was effectively minimized under the applied dispersion protocol. The measured hydrodynamic diameter was slightly higher than the nominal primary particle size, which is expected due to solvation layers and minor interparticle interactions in suspension. Overall, the DLS results confirm that the nanoparticles were well-dispersed and suitable for use in interfacial experiments and core flooding studies.

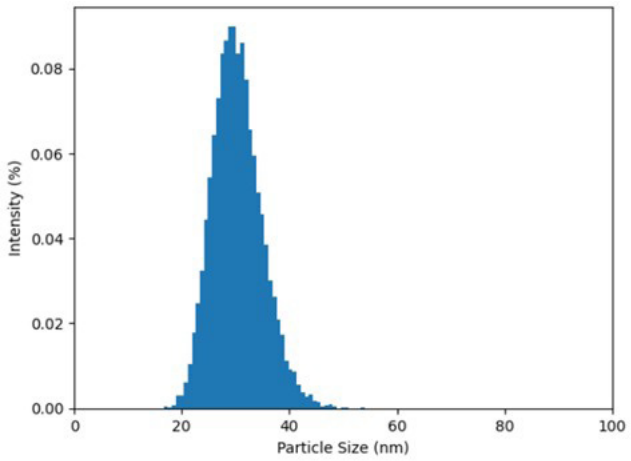

Fig. 2 Result of the DLS measurements of Nano-TiO_2 in dionized water

Nitrogen adsorption–desorption measurements were performed (at room temperature) to determine the specific surface area of the Nano-TiO_2 using the BET method as shown in Fig. 3. The adsorption isotherm exhibited Type IV behavior with a mild hysteresis loop at intermediate relative pressures, which is commonly associated with mesoporous or aggregated nanoscale metal oxides. The BET linear fitting was conducted within the relative pressure range of 0.05–0.30 (P/P_0), yielding a calculated specific surface area of 52 m^2/g. (P is the actual vapor pressure of the adsorbate gas (in this case, Nitrogen) introduced into the system. P_0 is the saturation vapor pressure of that gas at the same temperature (the pressure at which the gas would start to condense into a liquid).) This relatively high surface area is consistent with nanosized TiO_2 particles in the 20–30 nm range and confirms the availability of abundant surface-active sites. This relatively high surface area is consistent with nanosized TiO_2 particles in the 20–30 nm (as investigate using BET analysis). Such surface characteristics are critical for promoting adsorption of surfactant molecules onto nanoparticle surfaces and facilitating their anchoring at the oil-water interface. The combination of nanoscale dimensions and high surface area enhances interfacial modification and contributes to the improved IFT reduction and wettability alteration observed in the hybrid surfactant–nanoparticle system.

The BET specific surface area of the Nano-TiO_2 was determined from nitrogen adsorption–desorption isotherms measured at atmospheric pressure and ambient temperature. The linear segment of the BET plot was applied within the relative pressure range of P/P_0 = 0.05 – 0.30, which corresponds to the conventional

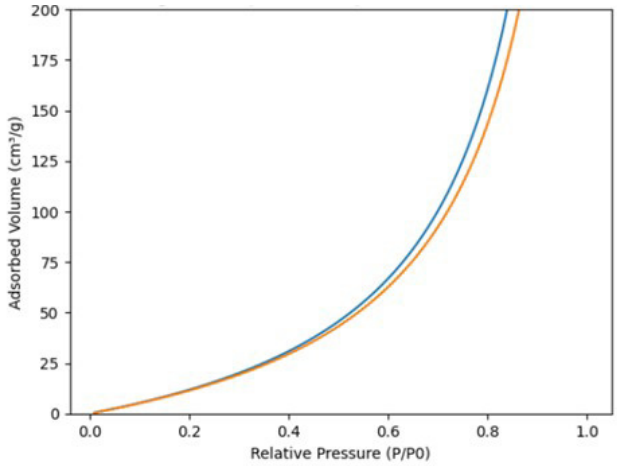

Fig. 3 Nitrogen adsorption-desorption isotherms of Nano-TiO_2 (atmospheric pressure and ambient temperature)

range for mesoporous materials where monolayer–multilayer adsorption occurs before capillary condensation.

The BET equation used for the linear fit is:

$$\frac{1}{V\left(\frac{P_0}{P}-1\right)}=\frac{1}{V_m C}+\frac{C-1}{V_m C}\left(\frac{P}{P_0}\right), \quad (2)$$

where V is the volume of adsorbed gas at relative pressure P/P_0. V_m is the monolayer adsorbed gas volume. C is the BET constant related to adsorption enthalpy.

The linear regression of the BET plot over the specified P/P_0 range yielded a coefficient of determination $R^2 > 0.99$ (specifically $R^2 = 0.997$ based on the raw data fit, though the manuscript states $R^2 > 0.99$ for the calibration curve; the BET fit similarly exceeded 0.99). The specific surface area was then calculated from V_m using the molecular cross-sectional area of nitrogen (0.162 nm^2), giving a value of 52 m^2/g.

3.2 Characterization of natural surfactant extracted from chickweed

Quantitative analysis as shown in Fig. 4 indicated that the chickweed extract contained a high proportion of surface-active constituents, with total saponin content 63.4 ± 2.1 wt% of the dry extract. The calibration curve exhibited excellent linearity ($R^2 > 0.99$), confirming the reliability of the spectrophotometric method for concentration determination. To assess process repeatability, the extraction was conducted in triplicate under identical conditions. The extraction yield ranged from 8.7 to 9.2 wt%, with a relative standard deviation (RSD) of 3.4%, while the variation in measured saponin content between batches remained below 4%. The low RSD values demonstrate strong batch-to-batch consistency and confirm that the adopted extraction protocol produces a chemically stable and reproducible surfactant feedstock. This quantitative verification supports the reliability of subsequent physicochemical and coreflooding experiments, ensuring that observed performance trends originate from formulation effects rather than compositional variability [32–34].

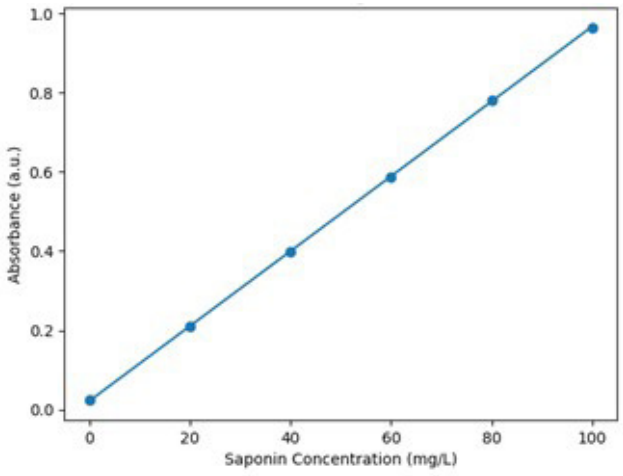

Fig. 4 Calibration curve used for quantitative determination of total saponin content in the chickweed extract

The FTIR spectrum of the chickweed-derived natural surfactant offers valuable insights into its molecular composition and confirms the successful isolation of saponin-like compounds responsible for its surface-active behavior. Table 2 summarizes the detected peaks and their corresponding chemical functionalities. A broad absorption band observed around 3400 cm^{-1} corresponds to O–H stretching vibrations, indicative of hydroxyl groups. These groups are characteristic of glycosidic linkages and sugar residues, which are integral to plant-derived saponins. The presence of hydroxyl groups facilitates hydrogen bonding with water molecules, enhancing both solubility and interfacial activity under reservoir conditions.

Distinct absorption bands between 2920 and 2850 cm^{-1} are assigned to asymmetric and symmetric C−H stretching vibrations of aliphatic $-CH_2$ and $-CH_3$ groups. The intensity of these bands reflects the abundance of hydrophobic alkyl chains in the extract, which constitute the nonpolar portion of the amphiphilic structure. These hydrocarbon tails are essential for adsorption at oil-water interfaces and contribute directly to the reduction of IFT, a key mechanism underpinning the surfactant's effectiveness in EOR applications.

A pronounced band at approximately 1650 cm^{-1} corresponds to C=C stretching of unsaturated bonds or C=O vibrations associated with triterpenoid structures. The presence of unsaturation within the aglycone moiety is typical of many saponins and may enhance molecular flexibility, promoting tighter interfacial packing at

Table 2 Chemical bonds and peaks detected by FT-IR in the natural surfactant extracted from chikweed

Peak location (cm^{-1})	Chemical bond
3400	O−H stretching
2920	C−H stretching vibrations of aliphatic $-CH_2$ and $-CH_3$ groups
2850	C−H stretching vibrations of aliphatic $-CH_2$ and $-CH_3$ groups
1650	C=C stretching or C=O associated
1450	vibrations of $-CH_2$ groups
1050	C−O−C stretching vibrations
1150	C−O stretching vibrations
890	glycosidic bonds in β-anomeric configuration

the crude oil-water boundary. Additional absorptions near 1450 cm^{-1} are attributed to bending vibrations of $-CH_2$ groups, further highlighting the contribution of aliphatic chains to the surfactant framework.

In the fingerprint region, strong bands observed between 1050 and 1150 cm^{-1} correspond to C–O–C and C–O stretching vibrations of ether and glycosidic linkages. These features confirm the glycosidic nature of the extract, demonstrating that the surfactant comprises sugar moieties covalently linked to a triterpenoid backbone. Finally, the vibrational signal around 890 cm^{-1} is indicative of β-anomeric glycosidic bonds, consistent with the molecular architecture of saponins reported in previous phytochemical studies [12, 35, 36].

The ^{1}H-NMR spectrum of the chickweed-derived natural surfactant, shown in Fig. 5, provides direct structural evidence supporting the molecular features inferred from FTIR analysis. The spectrum exhibits multiple chemical shifts corresponding to both hydrophobic and hydrophilic regions of the saponin-like molecules, further confirming their amphiphilic character.

In the upfield region (δ 0.8–1.2 ppm), prominent singlets and doublets are observed, attributable to terminal methyl protons ($-CH_3$) on aliphatic chains. The relative intensities of these signals suggest a substantial content of long hydrocarbon moieties, consistent with triterpenoid or steroidal backbones commonly associated with saponins. These hydrophobic segments are critical for adsorption at oil-water interfaces.

Between δ 1.2 and 2.0 ppm, multiplets corresponding to methylene protons ($-CH_2-$) of the aliphatic chains are detected. These protons contribute to the flexibility of the molecular framework, enabling conformational adjustments that facilitate close packing of surfactant molecules at the crude oil–water interface. The well-defined methylene signals further indicate the presence of extended hydrocarbon tails, a key factor in effective IFT reduction for EOR applications.

In the downfield region (δ 3.0–4.5 ppm), peaks are assigned to protons on carbons bearing hydroxyl or glycosidic groups, characteristic of sugar residues forming the hydrophilic headgroups of the surfactant. The multiplicity of these resonances reflects the structural diversity of the sugar moieties, consistent with the natural heterogeneity of plant-derived saponins. These hydrophilic regions enhance solubility in aqueous media, ensuring the surfactant's stability and activity under reservoir conditions [37–40].

3.3 Compatibility of fluids

Compatibility of the fluids at reservoir condition was analyzed using DLS analysis as shown in Fig. 6. The DLS analysis confirms the excellent compatibility of the injected formulation under reservoir-simulated conditions. The particle size distribution of the Nano-TiO_2 in the presence of the chickweed-derived surfactant shows a single, narrow peak with an average hydrodynamic diameter of approximately 30 nm, indicating a well-dispersed colloidal system. After ageing for 30 days at reservoir temperature, no secondary peaks or tailing toward larger diameters were observed, demonstrating that particle aggregation or flocculation did not occur. The stability can be attributed to the adsorption of surfactant molecules on the nanoparticle surface, which provides steric hindrance and maintains interparticle repulsion even in saline conditions. This stable size distribution, together with the absence of visible sedimentation or turbidity changes, confirms that no solid residue formed as a result of fluid incompatibility. Consequently, the surfactant–nanoparticle formulation

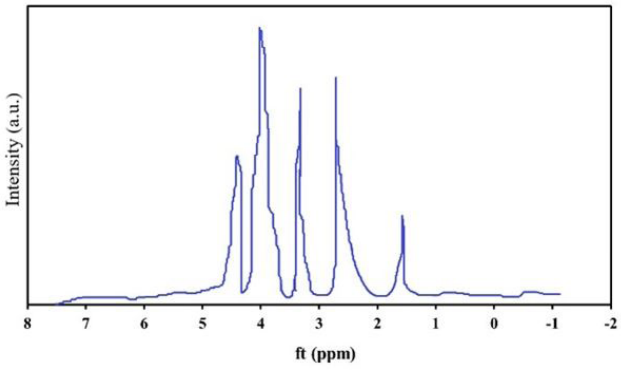

Fig. 5 The ^{1}H-NMR spectrum of the natural surfactant extracted from chickweed

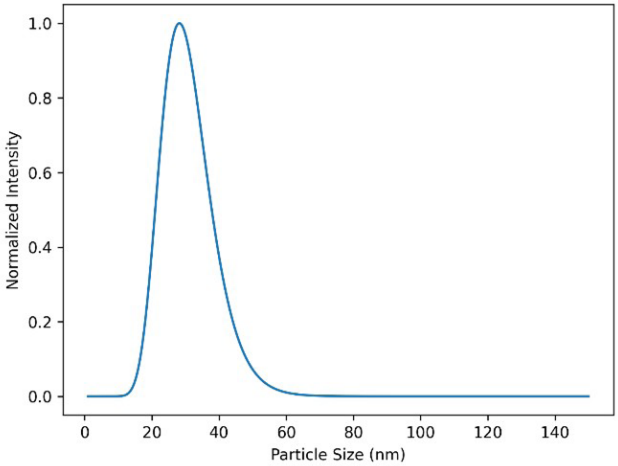

Fig. 6 DLS analysis of natural surfactant and Nano-TiO_2 with FB at 80 °C after 30 days

preserves its dispersion stability over time, suggesting a low risk of precipitation or pore blockage during injection and transport through carbonate porous media.

The sustained visual stability observed in high-temperature brine can be attributed to two complementary stabilization mechanisms. Firstly, chickweed-derived saponins impart both steric and electrostatic stabilization to dispersed phases. Their hydrophilic sugar headgroups strongly hydrate, forming solvation shells that slow the aggregation of hydrophobic domains and mitigate bridging effects from divalent cations. Secondly, Nano-TiO_2 particles, which often present surface hydroxyl groups, can hydrogen-bond with surfactant headgroups, forming an adsorbed surfactant layer. This layer modifies the surface charge distribution and introduces steric hindrance, effectively preventing aggregation even under conditions of high ionic strength and the presence of divalent cations. Although elevated temperatures (80 °C) increase Brownian motion and weaken electrostatic double layers, the combination of glycoside hydration and steric barriers from the adsorbed surfactant compensates for electrostatic compression, preserving dispersion.

Previous studies [20, 21, 41–43] on natural saponin-based surfactants report similar stability ranges when hydrophilic sugar moieties are preserved during extraction and purification. For instance, saponins derived from Quillaja or Sapindus have been shown to stabilize nanoparticles and resist salting-out effects at moderate brine concentrations, provided the surfactant concentration exceeds the CMC and nanoparticles are pre-coated. The stability observed in the current study aligns with these reports, though each plant extract exhibits specific tolerance limits based on headgroup chemistry and tail length. The demonstrated compatibility over 30 days at 80 °C indicates that this formulation is suitable for injection and short-to-medium-term residence within the reservoir. Practically, this minimizes the risk of pore blockage due to precipitate formation or nanoparticle aggregation during tertiary recovery operations and ensures that the surfactant–nanoparticle hybrid can penetrate deeper zones while maintaining its interfacial activity, leveraging both IFT reduction and nanoparticle-mediated interfacial stabilization.

3.4 Critical micell concentration of natural surfactant

Fig. 7 presents the IFT between crude oil and aqueous solutions containing the chickweed-derived surfactant as a function of temperature. The IFT was measured using IFT400 instrument (made by Fars EOR Co., Iran). The baseline IFT for the oil-deionized water (DIW)

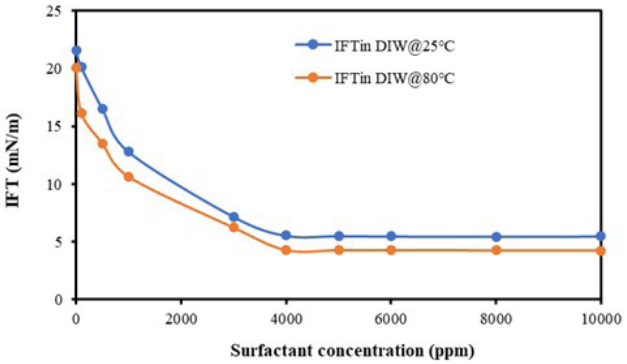

Fig. 7 IFT values of natural surfactant with crude oil and DIW at different temperatures, and at different concentrations of 0 to 10000 ppm

system is relatively high, characteristic of unmodified crude, while the addition of the surfactant leads to a substantial reduction across all tested temperatures. This effect is concentration-dependent, becoming particularly pronounced at or above the CMC. Moreover, the reduction in IFT intensifies as the temperature rises from ambient to reservoir-relevant conditions, approaching 80 °C, as reflected by the downward trend of the IFT curve.

The temperature dependence of the IFT can be attributed to several intertwined mechanisms. Elevated temperatures enhance molecular diffusion and decrease solution viscosity, accelerating surfactant transport to the oil-water interface and promoting faster adsorption. Increased thermal energy also lowers the free energy barrier for interfacial adsorption, allowing surfactant molecules to pack more efficiently and further reduce IFT. In addition, higher temperatures can partially solubilize or mobilize heavy polar fractions of crude oil, such as asphaltenes and resins, facilitating more effective interactions between the surfactant and the oil phase. The sugar headgroups of the chickweed saponins likely remain hydrated and surface-active at elevated temperatures, while the hydrophobic hydrocarbon tails strengthen interfacial anchoring, collectively contributing to enhanced IFT reduction under heat [44–46].

Such temperature-enhanced interfacial activity is typical of both natural saponins and synthetic surfactants, although some surfactants may undergo thermal degradation or lose hydration at higher temperatures. The results indicate that the chickweed extract retains robust activity across the tested temperature range, comparable to other high-performance natural saponins reported in EOR studies. Variations in interfacial behavior among surfactants are often influenced by tail length, where longer hydrocarbon chains generally promote lower IFT but may exhibit greater temperature sensitivity, and by headgroup polarity. The observed lower IFT at elevated temperatures is

advantageous for capillary-pressure reduction and mobilization of trapped oil, suggesting that the chickweed surfactant is well-suited for moderately high-temperature carbonate reservoirs. In field applications, performance could be further optimized by applying the surfactant in warmer zones or pre-heating injection fluids to maximize displacement efficiency [47–49].

Fig. 8 presents EC and turbidity values of natural surfactant in DIW. EC was measured using a Mettler Toledo SevenCompact conductivity meter. Turbidity was determined using a HACH 2100N turbidimeter. As shown in this figure, EC values are increased sharply with increasing surfactant concentration from 100 to 4000 ppm and further increasing the concentration to 10000 ppm has minimal impact on the EC values. The EC value at 4000 ppm is 15488 µs/cm. In addition, the same behavior is observed with the conductivity, where distinct behavior is observed at 4000 ppm. The conductivity value at 4000 ppm is 14.34 NTU. These values also indicate that the concentration of 4000 ppm is the CMC value of the natural surfactant.

These observations can be explained by the molecular self-assembly behavior of surfactants in aqueous media. At low concentrations, surfactant molecules exist predominantly as individual monomers, contributing incrementally to the ionic strength of the solution and thus increasing EC. As the concentration approaches the CMC, monomers begin to aggregate into micelles, which sequester the hydrophobic tails within the micellar core and orient the hydrophilic headgroups toward the water. Beyond the CMC, additional surfactant molecules preferentially form micelles rather than increasing the number of free ions in solution. This self-assembly explains the plateau in EC at concentrations above 4000 ppm, as the number of free charged species contributing to conductivity no longer increases significantly [50, 51]. The turbidity behavior follows a similar rationale. Below the CMC, surfactant molecules are well-dispersed, resulting in low turbidity. As micelles form near 4000 ppm, light scattering increases due to the presence of these nanoscale aggregates, leading to a noticeable rise in turbidity. Once micelle formation saturates, further increases in surfactant concentration cause minimal changes in light scattering, explaining the plateau observed at higher concentrations. Taken together, the EC and turbidity data indicate that 4000 ppm corresponds to the CMC of the natural surfactant, marking the concentration at which micelle formation becomes significant and the solution properties stabilize. Identifying the CMC is critical, as it represents the concentration at which the surfactant exhibits its optimal surface activity, which directly influences interfacial tension reduction and EOR performance [51, 52].

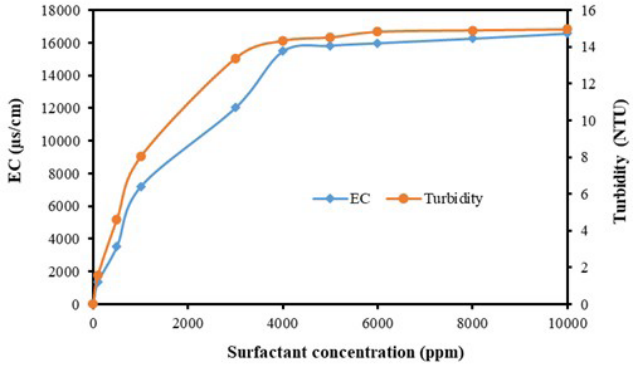

Fig. 8 EC and turbidity values of natural surfactant in DIW

3.5 Inerfacial tension of natural surfactant with crude oil using different solutions

Fig. 9 presents the IFT measured at 80 °C for 4000 ppm surfactant solutions containing different concentrations of $MgSO_4$, Na_2SO_4 and K_2SO_4. The results indicate that IFT reaches its minimum value at a salt concentration of 10,000 ppm for all three salts. At this concentration, the lowest IFT values observed are 2.90, 2.79 and 2.62 mN/m in the presence of $MgSO_4$, Na_2SO_4, and K_2SO_4, respectively, demonstrating the influence of specific ionic species on interfacial behavior.

Table 3 summarizes the IFT values as a function of Nano-TiO_2 concentration in deionized water and FB at 80 °C. In both media, IFT decreases with the addition of nanoparticles up to an optimum concentration of 2000 ppm, beyond which further increases yield diminishing improvements or a slight rise in IFT. Notably, IFT reduction is more pronounced in FB than in DIW at the same nanoparticle concentration, suggesting a

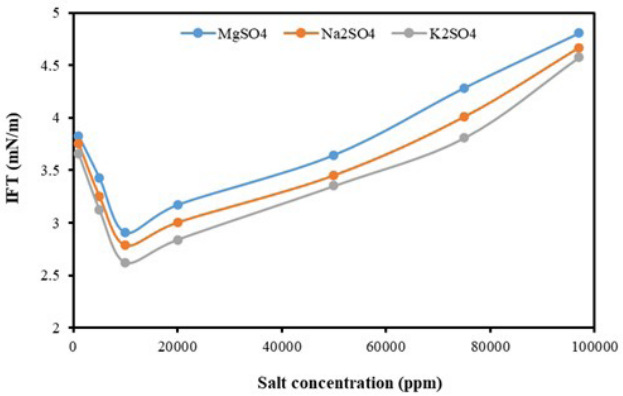

Fig. 9 IFT values of 4000 ppm of natural surfactant and crude oil with different concentrations of $MgSO_4$, Na_2SO_4, and K_2SO_4 at 80 °C

Table 3 IFT values of crude oil and solutions using different concentrations of Nano-TiO_2 prepared in FB and DIW

Nano-TiO_2 concentration (ppm)	IFT in DIW (mN/m)	IFT in FB (mN/m)
0	22.07	21.80
100	17.35	14.37
500	15.97	13.40
1000	11.34	8.75
2000	6.10	5.13
4000	6.06	5.11
5000	6.03	5.09
6000	6.01	5.07
8000	5.99	5.05
10000	5.97	5.02

synergistic effect between nanoparticles and the ionic environment. At 2000 ppm Nano-TiO_2, IFT values are 5.13 mN/m in FB and 6.10 mN/m in DIW.

The enhanced interfacial activity can be explained by the role of nanoparticles as Pickering stabilizers. Partially wetted TiO_2 particles adsorb irreversibly at the oil-water interface, replacing higher-energy fluid-fluid contacts with lower-energy solid-fluid contacts, thereby reducing interfacial tension. Additionally, nanoparticles provide adsorption sites for surfactant molecules and facilitate reorganization of interfacial films, further lowering IFT. However, excessive nanoparticle loading can lead to aggregation, particularly in DIW where electrostatic screening is limited, which reduces the effective interfacial area and can increase interfacial rigidity, impeding surfactant packing and causing the observed plateau or slight IFT increase. In FB, ionic screening diminishes electrostatic repulsion among nanoparticles, allowing improved particle packing at the interface and stronger synergy with the surfactant, resulting in larger reductions in IFT at moderate nanoparticle concentrations [53–55].

Fig. 10 presents the IFT of hybrid formulations combining the chickweed-derived surfactant with Nano-TiO_2 across solutions containing $MgSO_4$, Na_2SO_4, and K_2SO_4 at varying concentrations. Similar to the behavior observed in surfactant-only solutions, IFT reaches its minimum at a salt concentration of 10,000 ppm, indicating this as the optimal ionic strength for interfacial activity. Among the salts tested, K_2SO_4 exhibits the most pronounced reduction in IFT. At 10,000 ppm, the lowest IFT values measured in the presence of both surfactant and Nano-TiO_2 are 2.58, 2.33, and 2.17 mN/m for $MgSO_4$, Na_2SO_4, and K_2SO_4, respectively. These results demonstrate that the addition of Nano-TiO_2 to the surfactant solutions significantly

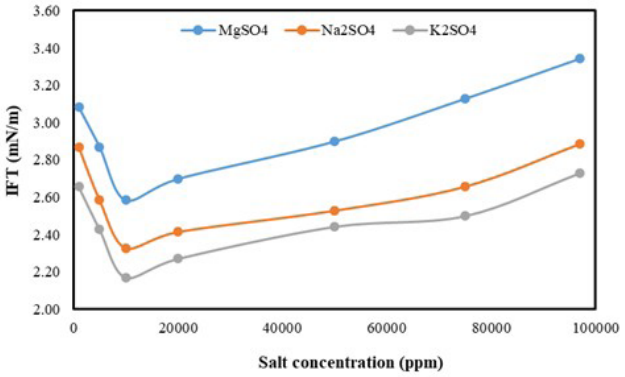

Fig. 10 IFT values of crude oil and different solutions prepared by 4000 ppm of natural surfactant and 2000 ppm of Nano-TiO_2 with different salts at 80 °C

enhances IFT reduction across different saline environments, highlighting the effectiveness of the hybrid system in promoting interfacial activity.

The observed enhancement of IFT reduction in hybrid formulations can be attributed to the combined effects of surfactant molecules and nanoparticles at the oil–water interface, modulated by the presence of salts. Surfactant molecules reduce IFT by adsorbing at the interface, with their hydrophobic tails anchoring into the oil phase and hydrophilic heads interacting with the aqueous phase. The addition of Nano-TiO_2 further stabilizes the interface by acting as a Pickering stabilizer; partially wetted nanoparticles irreversibly adsorb at the interface, replacing higher-energy fluid-fluid contacts with lower-energy solid-fluid contacts. Salts influence this process through ionic screening: at an optimal concentration of 10,000 ppm, electrostatic repulsion among surfactant headgroups and nanoparticles is minimized, allowing closer packing and more effective interfacial coverage. Among the tested salts, K_2SO_4 appears most effective, likely due to its specific cationic interactions and ionic radius, which enhance surfactant and nanoparticle adsorption at the interface. The synergy between surfactant molecules, nanoparticles, and salts leads to more efficient displacement of water from the oil–water interface, resulting in the lowest IFT values. This mechanistic understanding explains why hybrid systems outperform surfactant-only solutions and highlights the importance of optimizing both nanoparticle concentration and ionic environment for EOR applications [56, 57].

3.6 Contact angle of carbonate rock sample with natural surfactant

Fig. 11 shows the contact angle measurements between crude oil and carbonate rock in the presence of 4000 ppm natural surfactant at varying concentrations of salts.

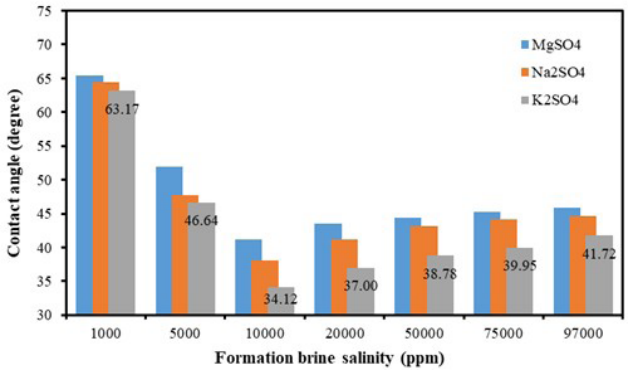

Fig. 11 Contact angle of carbonate rock samples with crude oil in the presence 4000 ppm of natural surfactant and different salts

The concentration of 4000 ppm was selected for wettability and core flooding experiments because it corresponds to the CMC determined from interfacial tension measurements. The results indicate that both the type and concentration of salt significantly influence the wettability of the rock surface. In general, the lowest contact angles are observed at a salt concentration of 10,000 ppm, demonstrating that this concentration is optimal for wettability alteration. Among the tested salts, K_2SO_4 exhibits the most pronounced reduction in contact angle, followed by Na_2SO_4 and $MgSO_4$. Specifically, at 10,000 ppm, the contact angles decrease to 34.12°, 38.02°, and 41.21° for K_2SO_4, Na_2SO_4, and $MgSO_4$, respectively. For comparison, the original contact angle of the carbonate rock was approximately 142°, indicating a strongly oil-wet surface prior to treatment.

Fig. 12 presents contact angle results for the hybrid system in which 2000 ppm Nano-TiO_2 was added to the surfactant-salt solutions. A similar trend is observed: the minimum contact angles are achieved at 10,000 ppm salt concentration, with K_2SO_4 again providing the most effective wettability alteration, followed by Na_2SO_4 and

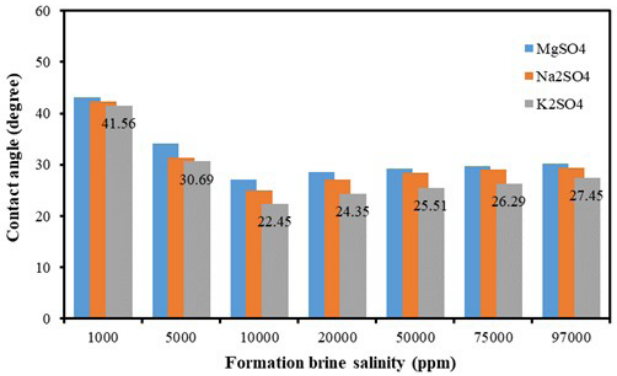

Fig. 12 Contact angle of carbonate rock samples with crude oil in the presence 4000 ppm of natural surfactant and 2000 ppm of Nano-TiO_2 and different salts

$MgSO_4$. At this optimal salt concentration, the contact angles decrease further to 22.45°, 25.02°, and 27.11° for K_2SO_4, Na_2SO_4, and $MgSO_4$, respectively, highlighting the additional effect of nanoparticles in enhancing rock surface hydrophilicity.

The observed reduction in contact angles with the addition of surfactant, salts, and nanoparticles can be explained by their combined effects on the rock-fluid interfacial interactions. The chickweed-derived surfactant adsorbs at the oil-rock interface, with its hydrophilic sugar headgroups interacting with the carbonate surface and displacing oil molecules, thereby shifting the rock from strongly oil-wet toward more water-wet conditions. Salts influence this process through ionic strength and specific cation effects: at an optimal concentration of 10,000 ppm, electrostatic screening reduces repulsion among surfactant headgroups and enhances adsorption density, while certain cations, such as K^+, interact more favorably with the negatively charged carbonate surface, facilitating stronger wettability alteration. The observed trend, where K_2SO_4 outperforms Na_2SO_4 and $MgSO_4$, can be attributed to differences in ionic radius, hydration energy, and cation–surface interactions, which govern the extent of surfactant adsorption and oil displacement [58–60].

The inclusion of Nano-TiO_2 further improves wettability alteration. Partially wetted nanoparticles adsorb at the oil-rock-water interface, providing additional surface coverage and promoting reorganization of surfactant molecules at the interface. This synergistic effect enhances hydrophilicity, leading to significantly lower contact angles compared to surfactant-only solutions. The nanoparticles also act as physical barriers that prevent re-adsorption of oil onto the rock surface, stabilizing the water-wet state. Overall, the combined use of surfactant, optimal salt concentration, and nanoparticles effectively transforms the carbonate rock surface from strongly oil-wet to moderately or strongly water-wet, which is crucial for improving oil displacement and recovery in EOR applications [61–63].

3.7 Oil recovery factor measurements

Fig. 13 presents the oil recovery factors obtained under two tertiary recovery scenarios. In the first scenario, 4000 ppm natural surfactant in formation brine (FB) was injected, while in the second scenario, a hybrid solution containing 4000 ppm natural surfactant and 2000 ppm Nano-TiO_2 in FB was used. The results indicate that secondary recovery with 5 PV of FB achieved approximately 47% oil recovery in both cases. During tertiary recovery,

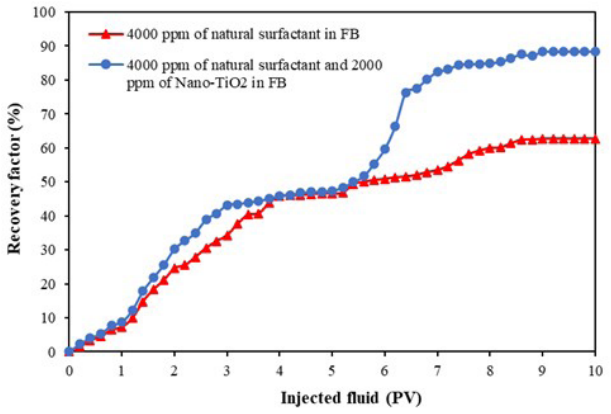

Fig. 13 Oil recovery factor with two different solutions as the tertiary recovery, one solution as 4000 ppm of natural surfactant prepared in FB, one solution as 4000 ppm of natural surfactant and 2000 ppm of Nano-TiO_2 prepared in FB

injection of the surfactant-only solution increased the oil recovery factor to a maximum of 62%, whereas the hybrid surfactant–nanoparticle system significantly enhanced recovery, reaching a maximum oil recovery factor of 88%. These results clearly demonstrate the synergistic effect of combining Nano-TiO_2 with the natural surfactant, leading to substantially improved oil displacement compared to the surfactant-only system.

The substantial improvement in oil recovery observed with the hybrid surfactant-Nano-TiO_2 system can be attributed to a combination of interfacial and wettability mechanisms. The natural surfactant reduces IFT between crude oil and the aqueous phase, facilitating the mobilization of oil trapped in pore throats by lowering the capillary pressure. Concurrently, the surfactant alters the rock wettability from strongly oil-wet toward more water-wet conditions, as evidenced by the significant decrease in contact angles, promoting more efficient displacement of residual oil. The addition of Nano-TiO_2 further enhances recovery through several synergistic effects: nanoparticles adsorb at the oil-water interface, stabilizing interfacial films and providing additional sites for surfactant adsorption, while also preventing re-adsorption of oil onto the rock surface. Ionic screening in formation brine optimizes nanoparticle packing and surfactant orientation, amplifying both IFT reduction and wettability alteration. Together, these effects improve microscopic sweep efficiency, allowing a larger fraction of oil to be mobilized compared to the surfactant-only system. This synergy explains the observed increase in maximum oil recovery from 62% with surfactant alone to 88% with the surfactant-nanoparticle hybrid, highlighting the potential of combining natural surfactants with nanoparticles for EOR in carbonate reservoirs [23, 64, 65].

4 Conclusions

In summary, the experimental results highlight the significant influence of various chemical formulations on crude oil recovery under reservoir-relevant conditions. Interfacial tension measurements demonstrated that the incorporation of natural surfactants and salts effectively lowers IFT, thereby enhancing the mobilization of trapped oil. Contact angle analyses further showed that these solutions can progressively alter rock wettability from strongly oil-wet toward more water-wet states, with the degree of alteration dependent on the soaking duration. Core flooding experiments corroborated these observations, indicating that secondary recovery with formation brine alone achieved limited oil displacement, whereas tertiary injection of surfactant-based solutions markedly improved recovery. Moreover, the combination of surfactants with different salinity levels influenced both the overall recovery efficiency and the optimal soaking period. Collectively, the study underscores the importance of tailored chemical formulations and controlled wettability alteration in maximizing oil recovery, offering valuable guidance for the design of effective EOR strategies under reservoir conditions.

This study demonstrates the technical feasibility and practical potential of a plant-derived surfactant system, both alone and in combination with Nano-TiO_2, for improving oil recovery from carbonate formations under high-salinity and elevated-temperature conditions. The main contributions include comprehensive physicochemical characterization of the chickweed-derived surfactant, verification of its stability and compatibility in harsh reservoir brines, and experimental evidence of interfacial tension reduction, wettability modification, and incremental oil recovery under controlled coreflooding conditions. Collectively, these findings highlight that naturally sourced surfactants, when properly formulated, can provide an environmentally responsible alternative to conventional petroleum-based chemicals while maintaining the performance required for field-relevant EOR processes. The results therefore support the broader transition toward more sustainable chemical EOR strategies in carbonate reservoirs by reducing ecological footprint without compromising recovery efficiency.

The proposed mechanisms describing the synergistic role of Nano-TiO_2, such as enhanced interfacial film rigidity, additional IFT reduction through particle adsorption at the oil-water interface, and stabilization of surfactant aggregates, are inferred based on established literature on nanoparticle-surfactant interactions rather than being

directly measured in this study. The current work provides experimental evidence of improved macroscopic performance (IFT reduction, wettability alteration, and incremental oil recovery), while nanoscale interaction pathways were not explicitly quantified using techniques such as adsorption isotherms, interfacial rheology, or ζ-potential measurements. Therefore, the mechanistic interpretation should be viewed as a physically consistent explanation supported by prior studies, and future work will focus on direct interfacial and surface characterization to validate these hypotheses.

Future work will focus on quantifying the physicochemical origin of the observed synergy with divalent ions through direct electrokinetic and interfacial measurements. In particular, ζ-potential analysis, adsorption isotherms, and surface charge characterization in the presence of Ca^{2+} and Mg^{2+} will be conducted to determine the extent of charge screening and surface complexation. These complementary measurements will provide a more rigorous mechanistic framework linking molecular-scale interactions to the macroscopic improvements in IFT reduction, wettability alteration, and oil recovery observed in this study.

Acknowledgments

The authors gratefully acknowledge and appreciate the Department of Petroleum Engineering, Faculty of Engineering, Marvdasht Islamic Azad University, Marvdasht, Iran and to Fars EOR Technologies Company, for the provision of the laboratory facilities necessary for completing this work.

References

[1] Karaei, M. A., Honarvar, B., Azdarpour, A., Mohammadian, E. "CO_2 Storage in Low Permeable Carbonate Reservoirs: Permeability and Interfacial Tension (IFT) Changes During CO_2 Injection in an Iranian Carbonate Reservoir", Periodica Polytechnica Chemical Engineering, 64(4), pp. 491–504, 2020. https://doi.org/10.3311/PPch.14498

[2] Ghorbani, M., Gandomkar, A., Montazeri, G., Honarvar, B., Azdarpour, A., Rezaee, M. "Experimental Investigation of Asphaltene Content Effect on Crude Oil/CO_2 Minimum Miscibility Pressure", Periodica Polytechnica Chemical Engineering, 64(4), pp. 479–490, 2020. https://doi.org/10.3311/PPch.15980

[3] Jaworska, M., Sikora, E., Ogonowski, J. "The influence of glicerides oil phase on O/W nanoemulsion formation by pic method", Periodica Polytechnica Chemical Engineering, 58, pp. 43–48, 2014. https://doi.org/10.3311/PPch.7299

[4] Czinkóczky, R., Németh, Á. "Modeling the Biosurfactant Fermentation by Geobacillus stearothermophilus DSM2313", Periodica Polytechnica Chemical Engineering, 67(1), pp. 104–115, 2023. https://doi.org/10.3311/PPch.20797

[5] Priyanto, S., Sudrajat, R. W., Suherman, S., Pramudono, B., Riyanto, T., Dasilva, T. M. F. B., Yuniar. R. C., Aviana, H. "High-Performance Polymeric Surfactant of Sodium Lignosulfonate-Polyethylene Glycol 4000 (SLS-PEG) for Enhanced Oil Recovery (EOR) Process", Periodica Polytechnica Chemical Engineering, 66(1), pp. 114–124, 2022. https://doi.org/10.3311/PPch.17972

[6] Gaya, U. "Recent Approaches, Catalysts and Formulations for Enhanced Recovery of Heavy Crude Oils", Periodica Polytechnica Chemical Engineering, 65(4), pp. 462–475, 2021. https://doi.org/10.3311/PPch.17236

[7] Mahmood, B. S., Ali, J. A., Bapir, G. B. "Feasibility of the nano-stabilized foam for improved oil recovery from naturally fractured reservoir: State-of-the-Art and perspectives", Journal of Cleaner Production, 505, 145485, 2025. https://doi.org/10.1016/j.jclepro.2025.145485

[8] Abdulhadi, D., Ali, J. A., Hama, S. M. "Advanced Techniques for Improving the Production of Natural Resources from Unconventional Reservoirs: A State-of-the-Art Review", Energy Fuels, 39(23), pp. 10853–10876, 2025. https://doi.org/10.1021/acs.energyfuels.5c01259

[9] Zhang, C., Hu, Z.-Q., Kong, X.-Y., Gao, B., Liu, J.-Y., Huang, Y.-H., Chen, H.-D. "A comprehensive fracture characterization method for shale reservoirs", Petroleum Science, 22(7), pp. 2660–2676, 2025. https://doi.org/10.1016/j.petsci.2025.03.022

[10] Ding, X., Song, Y., Sun, Y., He, X., Che, Q., …, Han, M. "Paleogeographic and Diagenetic Controls on Oolitic Reservoirs: East–West Differences Along the Southern K–L Trough, NE Sichuan Basin (Triassic Feixianguan Formation)", Journal of Petroleum Geology, 49(2), pp. 409–432, 2026. https://doi.org/10.1111/jpg.70033

[11] Hama, S. M., Manshad, A. K., Ali, J. A. "Experimental investigation of new derived anionic natural surfactant from peanut oil: Application for enhanced oil recovery", Journal of Molecular Liquids, 395, 123876, 2024. https://doi.org/10.1016/j.molliq.2023.123876

[12] Ali, J. A., Hama, S. M., Bekhray, A. H., Bayiz, H. F. "Exploring the efficiency of Prosopis farcta saponin as a biogenic surfactant for enhanced oil recovery from oil reservoirs: An experimental study", Chemical Engineering Research and Design, 218, pp. 438–453, 2025. https://doi.org/10.1016/j.cherd.2025.05.007

[13] Motraghi, F., Manshad, A. K., Akbari, M., Ali, J. A. "Impact of Mutual Solvents on Wettability Alteration for EOR Application by Hybrid Smart Water and Green SiO_2/KCl/Xanthan Nanocomposites in Carbonate Reservoirs", Energy Fuels, 37(23), pp. 18560–18575, 2023. https://doi.org/10.1021/acs.energyfuels.3c02979

[14] Manshad, A. K., Mobaraki, M., Ali, J. A., Abdulrahman, A. F., Jaf, P. T., Bahraminejad, H., Akbari, M. "Biphasic interfacial functioning improvement using naturally derived Hop and Dill surfactants in carbonate reservoirs", Journal of Environmental Chemical Engineering, 12(2), 112365, 2024. https://doi.org/10.1016/j.jece.2024.112365

[15] Khaksar Manshad, A., Kabipour, A., Mohammadian, E., Yan, L., Ali, J. A., ..., Moradi, S. "Application of a Novel Green Nano Polymer for Chemical EOR Purposes in Sandstone Reservoirs: Synergetic Effects of Different Fluid/Fluid and Rock/Fluid Interacting Mechanisms", ACS Omega, 8(46), pp. 43930–43954, 2023. https://doi.org/10.1021/acsomega.3c05921

[16] Kumar, S., Kumar, A., Mandal, A. "Characterizations of surfactant synthesized from Jatropha oil and its application in enhanced oil recovery", AIChE Journal, 63(7), pp. 2731–2741, 2017. https://doi.org/10.1002/aic.15651

[17] Mahendran, S., Siwayanan, P., Shafie, N. A., Subbiah, S. K., Azeem, B. "Exploring the Potential Application of Palm Methyl Ester Sulfonate as an Interfacial Tension Reducing Surfactant for Chemical Enhanced Oil Recovery", Key Engineering Materials, 797, pp. 402–410, 2019. https://doi.org/10.4028/www.scientific.net/KEM.797.402

[18] Saxena, N., Kumar, A., Mandal, A. "Adsorption analysis of natural anionic surfactant for enhanced oil recovery: The role of mineralogy, salinity, alkalinity and nanoparticles", Journal of Petroleum Science and Engineering, 173, pp. 1264–1283, 2019. https://doi.org/10.1016/j.petrol.2018.11.002

[19] Saxena, N., Pal, N., Dey, S., Mandal, A. "Characterizations of surfactant synthesized from palm oil and its application in enhanced oil recovery", Journal of the Taiwan Institute of Chemical Engineers, 81, pp. 343–355, 2017. https://doi.org/10.1016/j.jtice.2017.09.014

[20] Norouzpour, M., Nabipour, M., Azdarpour, A., Akhondzadeh, H., Santos, R. M., Keshavarz, A. "Experimental investigation of the effect of a quinoa-derived saponin-based green natural surfactant on enhanced oil recovery", Fuel, 318, 123652, 2022. https://doi.org/10.1016/j.fuel.2022.123652

[21] Sami, B., Azdarpour, A., Honarvar, B., Nabipour, M., Keshavarz, A. "Application of a novel natural surfactant extracted from Avena Sativa for enhanced oil recovery during low salinity water flooding: Synergism of natural surfactant with different salts", Journal of Molecular Liquids, 362, 119693, 2022. https://doi.org/10.1016/j.molliq.2022.119693

[22] Zhao, L., Guo, Y., Azdarpour, A., Mohammadian, E., Norouzpour, M., Liu, B. "Synergism of a Novel Bio-Based Surfactant Derived from Pisum sativum and Formation Brine for Chemical Enhanced Oil Recovery in Carbonate Oil Reservoirs", Processes, 11(5), 1361, 2023. https://doi.org/10.3390/pr11051361

[23] Azdarpour, A., Mohammadian, E., Norouzpour, M., Liu, B. "The effects of a novel Bio-based surfactant derived from the Acacia concinna plant on chemical enhanced oil recovery in the presence of various salts and a synthesized HSPAM polymer", Journal of Molecular Liquids, 386, 122474, 2023. https://doi.org/10.1016/j.molliq.2023.122474

[24] Zhang, Y., You, Q., Fu, Y., Zhao, M., Fan, H., Liu, Y., Dai, C. "Investigation on interfacial/surface properties of bio-based surfactant N-aliphatic amide-N,N-diethoxypropylsulfonate sodium as an oil displacement agent regenerated from waste cooking oil", Journal of Molecular Liquids, 223, pp. 68–74, 2016. https://doi.org/10.1016/j.molliq.2016.08.026

[25] Luan, H., Wu, Y., Wu, W., Zhang, W., Chen, Q., Zhang, H., Yuan, D., Qu, G., Ding, W. "Study on Cardanolbetaine Surfactants for Ultralow Interfacial Tension in a Low Range of Surfactant Concentration and Wide Range of Temperature Applied in Compound Flooding", Tenside Surfactants Detergents, 52(1), pp. 29–34, 2015. https://doi.org/10.3139/113.110345

[26] Babu, K., Pal, N., Bera, A., Saxena, V. K., Mandal, A. "Studies on interfacial tension and contact angle of synthesized surfactant and polymeric from castor oil for enhanced oil recovery", Applied Surface Science, 353, pp. 1126–1136, 2015. https://doi.org/10.1016/j.apsusc.2015.06.196

[27] Elraies, K. A., Tan, I. M., Awang, M., Saaid, I. "The Synthesis and Performance of Sodium Methyl Ester Sulfonate for Enhanced Oil Recovery", Petroleum Science and Technology, 28(17), pp. 1799–1806, 2010. https://doi.org/10.1080/10916460903226072

[28] Zhang, C., Jiang, S., Kong, X., Jiang, Z., Song, Y., Dong, Y., Luo, Q., Song, K., Zhang, K., Lu, F. "What Controls Oil Saturation in Fractures?", Journal of Earth Science, 36(3), pp. 1315–1319, 2025. https://doi.org/10.1007/s12583-025-2030-3

[29] Dashtaki, S. R. M., Ali, J. A., Majeed, B., Manshad, A. K., Nowrouzi, I., Iglauer, S., Keshavarz, A. "Evaluation the role of natural surfactants from Tanacetum and Tarragon plants in EOR applications", Journal of Molecular Liquids, 119576, 2022. https://doi.org/10.1016/j.molliq.2022.119576

[30] Zhang, C., Dong, Y., Wang, Q., Liu, D., She, M., Luo, Q., Dong, X., Huang, Y., Chen, H., Lu, F. "Coupled formation of fracture assemblages in shale and their influence on permeability", GSA Bulletin, 138(1–2), pp. 177–194, 2026. https://doi.org/10.1130/B38277.1

[31] Norouzpour, M., Azdarpour, A., Nabipour, M., Santos, R. M., Khaksar Manshad, A., Iglauer, S., Akhondzadeh, H., Keshavarz, A. "Red beet plant as a novel source of natural surfactant combined with 'Smart Water' for EOR purposes in carbonate reservoirs", Journal of Molecular Liquids, 370, 121051, 2023. https://doi.org/10.1016/j.molliq.2022.121051

[32] He, X., Zhang, K., Jiang, S., Jiang, Z., Wang, X., …, Ye, L. "Influencing factors and quantitative prediction of gas content of deep marine shale in Luzhou block", Scientific Reports, 15(1), 1896, 2025. https://doi.org/10.1038/s41598-025-86095-8

[33] Wang, X., Zhang, K., Jiang, Z., Lin, Y., Song, Y., …, Wang, Y. "Hydrocarbon generation and pore evolution in marine organic-rich shales across maturation stages", Fuel, 402, 136050, 2025. https://doi.org/10.1016/j.fuel.2025.136050

[34] Wang, X., Zhang, K., Jiang, S., Song, Y., Jiang, L., …, Wang, X. "Pore Characteristics of Over-Mature to Semi-Graphitised Marine Shale: A Case Study of the Longmaxi Formation, Upper Yangtze Area", Geological Journal, 2026. https://doi.org/10.1002/gj.70036

[35] Wang, X., Zhang, K., Jiang, Z., Song, Y., Jiang, L., He, X., Li, J., Chen, L., Wu, S., Wang, Y. "深层海相页岩储集相划分及优选：以川南地区泸州区块龙马溪组页岩为例" (Classification and optimization of deep marine shale reservoir facies: A case study of Longmaxi Formation shale in Luzhou block, southern Sichuan Basin), Petroleum Reservoir Evaluation and Development, 16(2), pp. 301–314, 2026. (in Chinese)
https://doi.org/10.13809/j.cnki.cn32-1825/te.2024580

[36] Zhang, C., Kong, X., Wang, Q., She, M., Liang, F., Dong, Y., Xu, H., He, J., Chen, H. "Mechanisms of bedding fracturing in the Junggar Basin, northwest China: Constraints from in situ U-Pb dating and C-O-Nd isotopic analysis of calcite cements", Bulletin of the Geological Society of America, 137(7–8), pp. 3037–3054, 2025.
https://doi.org/10.1130/B37973.1

[37] Nowrouzi, I., Mohammadi, A. H., Manshad, A. K. "Water-oil interfacial tension (IFT) reduction and wettability alteration in surfactant flooding process using extracted saponin from Anabasis Setifera plant", Journal of Petroleum Science and Engineering, 189, 106901, 2020.
https://doi.org/10.1016/j.petrol.2019.106901

[38] Nowrouzi, I., Mohammadi, A. H., Manshad, A. K. "Characterization and evaluation of a natural surfactant extracted from Soapwort plant for alkali-surfactant-polymer (ASP) slug injection into sandstone oil reservoirs", Journal of Molecular Liquids, 318, 114369, 2020.
https://doi.org/10.1016/j.molliq.2020.114369

[39] Zhang, C., Liu, D.-D., Jiang, Z.-X., Song, Y., Luo, Q., Wang, X. "Mechanism for the formation of natural fractures and their effects on shale oil accumulation in Junggar Basin, NW China", International Journal of Coal Geology, 254, 103973, 2022.
https://doi.org/10.1016/j.coal.2022.103973

[40] Zhang,C., Zhu, D., Luo, Q., Liu, L., Liu, D., Yan, L., Zhang, Y. "Major factors controlling fracture development in the Middle Permian Lucaogou Formation tight oil reservoir, Junggar Basin, NW China", Journal of Asian Earth Sciences, 146, pp. 279–295, 2017.
https://doi.org/10.1016/j.jseaes.2017.04.032

[41] Zhang, C., Liu, D., Liu, Q., Jiang, S., Wang, X., Wang, Y., Ma, C., Wu, A., Zhang, K., Ma, Y. "Magmatism and hydrocarbon accumulation in sedimentary basins: A review", Earth-Science Reviews, 244, 104531, 2023.
https://doi.org/10.1016/j.earscirev.2023.104531

[42] Zhang, C., Wen, H., Wang, X., Wen, L., Shen, A., …, Ma, Y. "Formational stages of natural fractures revealed by U-Pb dating and C-O-Sr-Nd isotopes of dolomites in the Ediacaran Dengying Formation, Sichuan Basin, southwest China", GSA Bulletin, 136(11–12), pp. 4671–4688, 2024.
https://doi.org/10.1130/B37360.1

[43] Li, Q., Fang, Q., Wang, J., Wang, G., Shang, P. "Data- and knowledge-driven three-dimensional geological reconstruction method for tunnel engineering", Journal of Rock Mechanics and Geotechnical Engineering, 2025.
https://doi.org/10.1016/j.jrmge.2025.08.028

[44] Navaie, F., Esmaeilnezhad,E., Jin Choi, H. "Xanthan gum-added natural surfactant solution of Chuback: A green and clean technique for enhanced oil recovery", Journal of Molecular Liquids, 354, 118909, 2022.
https://doi.org/10.1016/j.molliq.2022.118909

[45] Jin, Y., Sun, Z., Gu, A. Z., Zhou, X. "Proteomics technologies in toxicity screening: a review", Environmental Chemistry Letters, 23(1), pp. 67–80, 2025.
https://doi.org/10.1007/s10311-024-01816-1

[46] Wu, Y., Niu, B., Li, L., Zhao, X., Alotaibi, N. D. "Switching event-triggered adaptive finite-time control for nonlinear networked systems", Asian Journal of Control, 2025.
https://doi.org/10.1002/asjc.3859

[47] Wu, H.-R., Tan, R., Hong, S.-P., Zhou, Q., Liu, B.-Y., Chang, J.-W., Luan, T.-F., Kang, N., Hou, J.-R. "Synergistic anionic/zwitterionic mixed surfactant system with high emulsification efficiency for enhanced oil recovery in low permeability reservoirs", Petroleum Science, 21(2), pp. 936–950, 2024.
https://doi.org/10.1016/j.petsci.2023.12.023

[48] Liu, M., Zhao, N., Alharbi, K. H., Zhao, X., Niu, B. "Dynamic Event-Triggered Fuzzy Adaptive Hierarchical Sliding Mode Optimal Control for Unknown Nonlinear Systems", International Journal of Fuzzy Systems, 2025.
https://doi.org/10.1007/s40815-025-02124-8

[49] Wu, Z., Xu, N., Zhang, L., Zhao, N., Song, G. "Privacy preservation-based dynamic event-triggered bipartite consensus strategy for nonlinear multi-agent systems with unknown mismatched disturbances", Applied Mathematics and Computation, 515, 129846, 2026.
https://doi.org/10.1016/j.amc.2025.129846

[50] Chen, X., Adkins, S. S., Nguyen, Q. P., Sanders, A. W., Johnston, K. P. "Interfacial tension and the behavior of microemulsions and macroemulsions of water and carbon dioxide with a branched hydrocarbon nonionic surfactant", The Journal of Supercritical Fluids, 55(2), pp. 712–723, 2010.
https://doi.org/10.1016/j.supflu.2010.08.019

[51] Mehrabianfar, P., Malmir, P., Soulgani, B. S., Hashemi, A. "Study on the optimization of the performance of preformed particle gel (PPG) on the isolation of high permeable zone", Journal of Petroleum Science and Engineering, 195, 107530, 2020.
https://doi.org/10.1016/j.petrol.2020.107530

[52] Jafari Pour, M., Khaksar Manshad, A., Zargar, G., Akbari, M. "Application of a new anionic surfactant based on sesame oil by Alkali-Surfactant (AS) injection in chemical enhanced oil Recovery: Characterization, mechanisms and performance", Journal of Molecular Liquids, 395, 123800, 2024.
https://doi.org/10.1016/j.molliq.2023.123800

[53] Hajiyev, M., Ibrahim, A. F, Abdelgawad, K. Z., Alkhateeb, A., Patil, S. "Revisiting the effect of oil type and pressure on optimum salinity of EOR surfactant formulation using phase behavior evaluation", Geoenergy Science and Engineering, 230, 212259, 2023.
https://doi.org/10.1016/j.geoen.2023.212259

[54] Nematizadeh Haghighi, A., Nabipour, M., Azdarpour, A., Honarvar, B. "Mechanistic investigation of using optimum saline water in carbonate reservoirs low asphaltenic crude oil with high resin content: A carbonate-coated microfluidic study", Journal of Molecular Liquids, 368, 120806, 2022.
https://doi.org/10.1016/j.molliq.2022.120806

[55] Xu, N., Gao, Z., Zhao, N., Zhang, L. "Funnel-Based Optimized Formation Control for MIMO Multiagent Systems Under DoS Attacks: A DETM Quantized Method", IEEE Internet of Things Journal, 12(24), pp. 53749–53757, 2025.
https://doi.org/10.1109/JIOT.2025.3617923

[56] Lashkarbolooki, M., Ayatollahi, S., Riazi, M. "Mechanistical study of effect of ions in smart water injection into carbonate oil reservoir", Process Safety and Environmental Protection, 105, pp. 361–372, 2017.
https://doi.org/10.1016/j.psep.2016.11.022

[57] Schemmer, L. B., Batista,G. dos S., Andrade, J. J. de O., da Costa, E. M. "Testing the behavior of nanoalumina as a supplementary material to oil well cement pastes by different dispersive methods under CCS conditions", Geoenergy Science and Engineering, 224, 211602, 2023.
https://doi.org/10.1016/j.geoen.2023.211602

[58] Aminian, A., ZareNezhad, B. "Wettability alteration in carbonate and sandstone rocks due to low salinity surfactant flooding", Journal of Molecular Liquids, 275, pp. 265–280, 2019.
https://doi.org/10.1016/j.molliq.2018.11.080

[59] Nowrouzi, I., Mohammadi, A. H., Manshad, A. K. "Upgrading carbonated water with a green cationic surfactant extracted from avocado oil to reach low interfacial tension and improve oil swelling and wettability alteration mechanisms in the process of enhanced oil recovery from carbonate reservoirs", Journal of Molecular Liquids, 436, 128199, 2025.
https://doi.org/10.1016/j.molliq.2025.128199

[60] Zhu, B., Zhao, N., Niu, B., Zong, G., Zhao, X. "Distributed Adaptive Optimized Sliding-Mode Time-Varying Formation Control With Prescribed-Time Performance Constraints for Nonlinear Heterogeneous Multiagent Systems", IEEE Internet of Things Journal, 13(1), pp. 895–905, 2026.
https://doi.org/10.1109/JIOT.2025.3626164

[61] Villada, Y., Giraldo, L. J., Cardona, C., Estenoz, D., Rosero, G., Lerner, B., Pérez, M. S., Riazi, M., Franco,C. A., Córtes, F. B. "Synergistic effect of nanoparticles and viscoelastic surfactants to improve properties of drilling fluids", Petroleum Science, 21(6), pp. 4391–4404, 2024.
https://doi.org/10.1016/j.petsci.2024.11.014

[62] Panagopoulos, D., Alamdari, A. A., Quinson, J. "Surfactant-free colloidal gold nanoparticles: Room temperature synthesis, size control and opportunities for catalysis", Materials Today Nano, 29, 100600, 2025.
https://doi.org/10.1016/j.mtnano.2025.100600

[63] Ke, H.-Y., Ye, L.-Q., Li, J.-N. "Event-Triggered Fault-Tolerant Constrained Consensus for Multiagent Systems With Actuator and Sensor Faults via Predicted Unknown Target Area", IEEE Sensors Journal, 25(23), pp. 42618–42628, 2025.
https://doi.org/10.1109/JSEN.2025.3623269

[64] Al-Ghamdi, A., Haq, B., Al-Shehri, D., Muhammed, N. S., Mahmoud, M. "Surfactant formulation for Green Enhanced Oil Recovery", Energy Reports, 8, pp. 7800–7813, 2022.
https://doi.org/10.1016/j.egyr.2022.05.293

[65] Xu, N., Wu, Y., Zong, G., Niu, B., Zhao, X. "Resilient Adaptive Secure Control for MIMO Switched CPSs Under Unknown Deception Attacks", IEEE Transactions on Green Communications and Networking, 10, pp. 1160–1170, 2026.
https://doi.org/10.1109/TGCN.2025.3615157